Summary: Sequential crystallization of poly(L-lactide) (PLLA) followed by poly(ε-caprolactone) (PCL) in double crystalline PLLA-*b*-PCL diblock copolymers is studied by differential scanning calorimetry (DSC), polarized optical microscopy (POM), wide-angle X-ray scattering (WAXS) and small-angle X-ray scattering (SAXS). Three samples with different compositions are studied. The sample with the shortest PLLA block (32 wt.-% PLLA) crystallizes from a homogeneous melt, the other two (with 44 and 60% PLLA) from microphase separated structures. The microphase structure of the melt is changed as PLLA crystallizes at 122 °C (a temperature at which the PCL block is molten) forming spherulites regardless of composition, even with 32% PLLA. SAXS indicates that a lamellar structure with a different periodicity than that obtained in the melt forms (for melt segregated samples). Where PCL is the majority block, PCL crystallization at 42 °C following PLLA crystallization leads to rearrangement of the lamellar structure, as observed by SAXS, possibly due to local melting at the interphases between domains. POM results showed that PCL crystallizes within previously formed PLLA spherulites. WAXS data indicate that the PLLA unit cell is modified by crystallization of PCL, at least for the two majority PCL samples. The PCL minority sample did not crystallize at 42 °C (well below the PCL homopolymer crystallization temperature), pointing to the influence of pre-crystallization of PLLA on PCL crystallization, although it did crystallize at lower temperature. Crystallization kinetics were examined by DSC and WAXS, with good agreement in general. The crystallization rate of PLLA decreased with increase in PCL content in the copolymers. The crystallization rate of PCL decreased with increasing PLLA content. The Avrami exponents were in general depressed for both components in the block copolymers compared to the parent homopolymers.

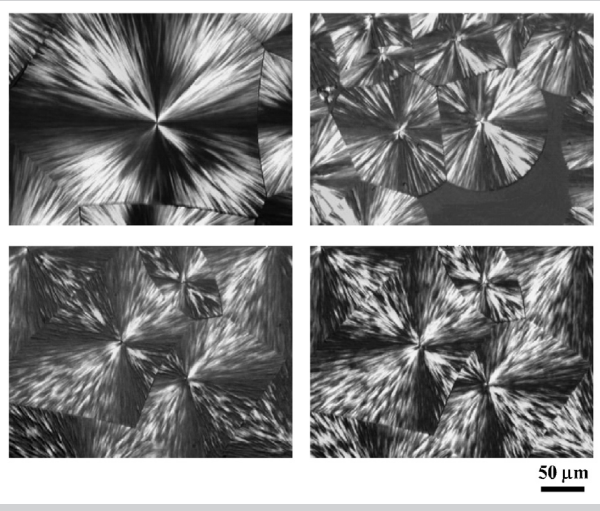

Polarized optical micrographs during isothermal crystallization of (a) homo-PLLA, (b) homo-PCL, (c) and (d) block copolymer after 30 min at 122 °C and after 15 min at 42 °C.

Melt Structure and its Transformation by Sequential Crystallization of the Two Blocks within Poly(L-lactide)-*block*-Poly(ε-caprolactone) Double Crystalline Diblock Copolymers

I. W. Hamley,[*1] P. Parras,[1] V. Castelletto,[1] R. V. Castillo,[2] A. J. Müller,*[*2] E. Pollet,[3] P. Dubois,[3] C. M. Martin[4]

[1] School of Chemistry, University of Reading, Whiteknights, Reading RG6 6AD, UK
E-mail: ian.hamley@talk21.com
[2] Departamento de Ciencia de los Materiales, Universidad Simón Bolívar, Apartado 89000, Caracas 1080-A, Venezuela
E-mail: muller@ush.ve
[3] Service des Materiaux Polymeres et Composites SMPC, Universite de Mons-Hainaut, Place du Parc 20, B-7000 Mons, Belgium
[4] Synchrotron Radiation Source, CLRC Daresbury Laboratory, Warrington WA4 4AD, UK

Received: February 24, 2006; Revised: March 31, 2006; Accepted: April 3, 2006; DOI: 10.1002/macp.200600085

Keywords: block copolymers; crystallization; differential scanning calorimetry (DSC); polarized optical microscopy (POM); SAXS

Introduction

Block copolymers have the remarkable ability to self-assemble in the melt into a variety of ordered structures with nanoscale periodicities, via microphase separation. These structures can be controlled by varying the composition of the block copolymer or the segregation between blocks.[1] In cases where one or more blocks can crystallize, the crystallization is accompanied by profound structural and dynamic changes that may compete with phase segregation. Crystallization can be either confined within the copolymer microdomain structure for strongly segregated systems, or it can drive structure formation for weakly segregated melts (overwriting any previous microdomain structure) or homogeneous systems. Several recent reviews deal with the properties of semi-crystalline block copolymers.[2–4] Although there have been a number of prior reports on double crystalline diblock copolymer systems, the understanding of their complicated properties is still at a nascent stage.[5–16]

Poly(L-lactide) (PLLA) has been widely employed in the medical field because of its biodegradability. However the applications of PLLA to commercial products are limited principally by its brittleness. This weakness might be improved if a polymer with a lower glass transition temperature is employed to prepare blends or is copolymerized with PLLA. A natural choice is poly(ε-caprolactone) (PCL) since it is also biodegradable and has a T_g of −65 °C. Since PLLA with a high molecular weight is reported to be immiscible with PCL,[17–19] the morphology of PLLA/PCL blends would be coarse and with low adhesion strength, thus desirable mechanical properties are not anticipated. On the other hand, PLLA-*b*-PCL block copolymers cannot macroscopically phase segregate and exhibit various microdomain structures at the nanoscale depending upon the block length ratio between the blocks. The mechanical properties as well as biodegradability are very much affected by the crystallinity of the constituent blocks that in turn depends upon the microdomain structure.[6,20]

Jeon et al.[21] prepared polydisperse multiblock PLLA-*b*-PCL and triblock PLLA-*b*-PCL-*b*-PLLA copolymers. They reported that the multiblock and triblock copolymers were phase separated in the melt since they found a single small angle X-ray scattering (SAXS) reflection that they interpreted as arising from the diffraction of poorly ordered spherical or hexagonally packed cylinders for multiblock copolymers and lamellar microdomains for triblock copolymers (they did not observe higher order peaks in their SAXS measurements). Aditionally, a spherulitic morphology was found regardless of composition for all copolymers examined.

Ho et al.[9] have roughly estimated that χN for PLLA-*b*-PCL diblock copolymers is in the range 2.9–4 (at temperatures between 180 and 50 °C) for samples with $\overline{M}_n$ values of 23 600 g · mol^{-1}. Since these χN values are quite low in comparison with the expectation of the mean field theory for block copolymers in the weak segregation regime, it is expected that the crystallization proceeds from a mixed melt. Furthermore, the morphology obtained for a PLLA-*b*-PCL diblock copolymer containing 72% PLLA (by tapping-mode scanning probe microscopy (SPM) for a spin-coated thin film quenched from 170 °C) was consistent with crystallization from a melt mixed system.[9] However, the calculation of Flory's interaction parameter through the equation $\chi = V_u(\delta_{PCL} - \delta_{PLA})^2/RT$ (where V_u is a reference volume, R is the universal gas constant, T is the absolute temperature and δ_p is the solubility parameter of polymer p) is highly dependent on the values of the solubility parameters. Ho et al. employed a value of $\delta_{PLA} = 9.79$ (cal · cm^{-3})$^{1/2}$ however, reported values in the order of 10–11 (cal · cm^{-3})$^{1/2}$ have also been reported in the literature[22] and these can yield values for χN of 11–50 depending on the molecular weight and temperature range considered.

Maglio et al.[10] found by dynamic mechanical thermal analysis (DMTA) that a PLLA-*b*-PCL-*b*-PLLA triblock copolymer (of composition 40/20/40, $\overline{M}_n = 49\,000$ g · mol^{-1} and a polydispersity index of 1.32) exhibited two glass transition temperatures at almost the same values as those found for the equivalent homopolymers. Therefore, they concluded that the two blocks were immiscible.

Kim et al.[6] reported on the synthesis and characterization of PLLA-*b*-PCL diblock copolymers. They obtained polymers with polydispersities in the range of 1.3–1.6. They found a rheological T_{ODT} of 220 °C for two copolymers: one containing 32 wt.-% PCL with a $\overline{M}_n = 77\,000$ g · mol^{-1} and another with 46% PCL and $\overline{M}_n = 46\,000$ g · mol^{-1}. In the case of another sample containing 37.4 wt.-% PCL and 19 000 g · mol^{-1} they found a homogeneous melt just above the melting point of the PLLA block at 175 °C. In this last copolymer, they found some structure formation in the melt prior to crystallization as indicated by a SAXS peak whose intensity later decreased when the PLLA crystallization process advanced. Kim et al.[6] investigated the crystallization of the PLLA block only, since they employed high crystallization temperatures (T_c) at which the PCL block was molten. Table 1 summarizes previous experimental observations and their interpretation in these interesting materials.

In a previous study,[16] we have investigated the crystallization of two well defined PLLA-*b*-PCL diblocks, by time resolved X-ray techniques, polarized optical microscopy (POM) and differential scanning calorimetry (DSC). Two compositions were studied that contained 44 and 60 wt.-% poly(L-lactide), PLLA (they were referred to as: $L_{44}^{11}C_{56}^{14}$ and $L_{60}^{12}C_{40}^{9}$ respectively with the molecular weight of each block in kg · mol^{-1} as superscript). The copolymers appeared to be initially miscible in the melt

Table 1. Melt behavior of different PLLA-*b*-PCL block copolymers reported in the literature.

Authors	PLLA-PCL[a)]	$\bar{M}_n$ / g · mol^{-1}	I[b)]	Melt Morphology
Ho et al.[9]	72/28	23 600	1.2	Disordered phase at $T = 170$ °C, observed by SPM. Formation of nanopatterned microdomains using different crystalline substrates were reported.
Kim et al.[6]	63/37	19 000	1.4	Homogeneous just above the melting point at $T = 175$ °C, observed by rheological measurements. However, they found some structure formation in the melt prior to crystallization as indicated by a SAXS peak.
Kim et al.[6]	54/46	46 000	1.3	Heterogeneous up to $T_{ODT} = 220$ °C. They considered that this block copolymer is weakly segregated at 190 °C.
Kim et al.[6]	68/32	77 000	1.6	Microphase-separated structure up to $T = 220$ °C, obtained by rheological measurements. Also, they reported a spherulitic morphology during PLLA crystallization quenching from 190 °C.
Maglio et al.[10]	40/20/40	49 000	1.3	Immiscible, as the copolymer T_gs are nearly identical to those of the homopolymer, determined by DMTA.
Jeon et al.[21]	triblock	50 600	1.9	Lamellar structure because of microphase separation, revealed by a single reflection in their SAXS profiles. The crystalline morphologies were spherulitic, irrespective of the PCL block length.
Hamley et al.[16]	60/40	20 900	1.1	Miscible in the melt at 190 °C, however time-resolved SAXS experiments revealed that upon cooling from the melt the sample transformed into a transient microphase-separated lamellar structure just before crystallization of PLLA block started.
Hamley et al.[16]	44/56	25 300	1.3	Miscible in the melt at 190 °C according to SAXS measurements.

a) PLLA-*b*-PCL copolymer composition.
b) Polydispersity index of the final copolymer.

according to SAXS. However, time-resolved SAXS experiments on $L^{12}_{60}C^{9}_{40}$ revealed an initial melt mixed morphology at 165 °C that upon cooling transformed into a transient microphase separated lamellar structure prior to crystallization at 100 °C. Sequential isothermal crystallization from the melt at 100 °C (for 30 min) and then at 30 °C (for 15 min) was examined. At 100 °C only the PLLA block was capable of crystallization and its crystallization kinetics was followed by both wide angle X-ray scattering (WAXS) and DSC and comparable results were obtained that indicated an instantaneous nucleation with three dimensional superstructures (Avrami index of approximately 3). The spherulitic nature of the superstructure was confirmed by POM, both PCL and PLLA formed negative spherulites. When the temperature was decreased to 30 °C, the PCL block was able to crystallize within PLLA negative spherulites (with an Avrami index of 2, as opposed to 3 in homo-PCL) and its crystallization rate was much slower than an equivalent homo-PCL.

In the present work we made new experiments employing the same samples as before ($L^{11}_{44}C^{14}_{56}$ and $L^{12}_{60}C^{9}_{40}$) plus an additional one (i.e., $L^{7}_{32}C^{15}_{68}$) in order to assess in detail the structure of the melt by SAXS (as a function of composition) and whether or not changes in structure occur upon cooling from the melt and before and after crystallization. The addition of a new copolymer which is within the same molecular weight range as the others but with a different composition has added new insight to the composition dependence. This together with the new annealing protocol applied to all 3 samples has uncovered very interesting new results about the structure of the melt and its subsequent transformation upon crystallization of each component plus the composition dependence of the effect. Furthermore the optical microscopy studies on the new block copolymer sample have also added novel results; we show here that even with 32 wt.-% PLLA well developed PLLA spherulites can form at temperatures where the PCL block is molten. Upon cooling the sample, PCL crystallization occurs within the PLLA spherulites with very little modification of the superstructural morphology but with substantial modification at the lamellar and unit cell level as revealed by SAXS and WAXS. According to previous literature, PLLA-*b*-PCL block copolymers are either mixed in the melt or weakly segregated (and may exhibit transient phases before crystallization). In this work, extensive real time SAXS measurements on well defined PLLA-*b*-PCL diblock copolymers have been performed to ascertain the block copolymer microdomain structure. Additionally, sequential crystallization experiments by WAXS and DSC explore the crystallization kinetics and the influence of the

Table 2. Molecular characteristics of the block copolymers and homopolymers.

Sample code	PLLA/PCL exp. comp.[a)]	$\bar{M}_{n,exp}$[b)] PLLA block	$\bar{M}_{n,exp}$[c)] PCL block	I[d)]
PLLA[24]	100/0	23 900	–	1.1
$L_{60}^{12}C_{40}^{9}$	60/40	12 400	8 500	1.1
$L_{44}^{11}C_{56}^{14}$	44/56	11 100	14 200	1.3
$L_{32}^{7}C_{68}^{15}$	32/68	6 900	14 900	1.4
PCL[29]	0/100	–	28 900	1.3

[a)] Experimental composition as determined by ^{1}H NMR.
[b)] Calculated $\bar{M}_n$ estimated by ^{1}H NMR for the PLLA block knowing the $\bar{M}_n$ of the PCL block determined by SEC.
[c)] Experimental $\bar{M}_n$ estimated by SEC for the PCL block.
[d)] Polydispersity index of the final copolymer (determined by SEC).

PLLA block crystallization on the PCL block crystallization.

Experimental Part

The block copolymers were synthesized by controlled/''living'' sequential block copolymerization as initiated by aluminum trialkoxides in toluene solution. These procedures were described in detail previously.[16,23] Table 2 lists the molecular weight characterization data obtained by size exclusion chromatography (SEC) and by ^{1}H NMR. The diblock copolymer nomenclature that we have used denotes the PLLA block as L and the PCL block as C, subscripts indicate the approximate composition in wt.-% and superscripts the approximate number average molecular weight in $kg \cdot mol^{-1}$.

All samples used in this paper were prepared by solvent evaporation from chloroform solutions. Additionally, PLLA/PCL blends were prepared by mixing homopolymer samples (whose molecular characteristics are also given in Table 2), with identical compositions to those of the block copolymers under study, in chloroform at 1% concentration. The solutions were left to dry in a fume hood for 2 d at room temperature and then transferred to a vacuum oven also at room temperature where they were dried until the achievement of a constant weight (one week).

SAXS/WAXS Measurements

Simultaneous small-angle and wide-angle X-ray scattering experiments were performed on station 6.2 at the Synchrotron Radiation Source, Daresbury Lab, UK.[24,25] Samples contained in DSC pans modified to incorporate mica windows to allow transmission of the X-ray beam were mounted in a Linkam DSC cell of single pan design for thermal treatment. The X-ray wavelength was $\lambda = 1.40$ Å. SAXS data were collected with a RAPID multiwire quadrant detector and the WAXS detector had a curved multiwire design. The wavenumber $q = 4\pi \sin\theta/\lambda$ for SAXS was calibrated using rat-tail collagen, and the WAXS angular scale was calibrated ''internally'' using the reflections from PLLA and PCL. This proved more reliable than using high density polyethylene (HDPE), which was also measured.

DSC Measurements

A Perkin-Elmer DSC-7 differential scanning calorimeter was employed. Samples were encapsulated in Aluminium pans (mass was approximately 5 mg in all cases). The calibration was performed with Indium and Hexatriacontane and all tests were run employing ultra pure nitrogen as purge gas. Standard DSC heating and cooling scans were performed at $10\,^{\circ}C \cdot min^{-1}$. Isothermal measurements were also performed, with a cooling rate equal to that used in SAXS/WAXS experiments. Tests were performed to check that the sample did not crystallize during cooling at a particular isothermal temperature.

POM Measurements

Thin films were prepared between microscope cover slips by melting the polymer at 190 °C for 3 min and then quickly cooling to the isothermal crystallization temperature in a Linkam TP-91 hot-stage. The samples were observed between crossed polarizers in a Zeiss MC-80 optical microscope equipped with a camera system. In order to enhance contrast and determine the sign of the spherulites, a λ wave plate was inserted between the polarizers.

Results and Discussion

Standard DSC Results

Figure 1 presents cooling scans from the melt (samples were first heated to 190 °C and kept at that temperature for 3 min, while Figure 2 shows immediate subsequent heating scans (all at $10\,^{\circ}C \cdot min^{-1}$). The peak crystallization temperatures in Figure 1 and the melting temperatures in Figure 2 are affected by composition as can be observed in Figure 3 and Table 3. Figure 3 also contains parallel data obtained for blends prepared in solution with the homopolymers (see experimental section). It is remarkable how the blends exhibit two crystallization and melting temperatures that are almost identical to those obtained for the parent homopolymers, a clear sign of immiscibility. It should be noted that the T_g of PLLA is located at around 50 °C (see Figure 2). However, in the blends and in the copolymers, the T_g is overlapped by the melting of the PCL phase and therefore it cannot be seen, so it is difficult to use T_g values as a miscibility criterion. The T_g of the PCL is located at −65 °C, outside the temperature range of the cooling device employed with our DSC. On the other hand, Figure 3 shows that the melting point (and the peak crystallization temperature) of the PLLA phase in the block copolymers is depressed as the content of PCL increases. This depression reaches a value of 11 °C for sample $L_{32}^{7}C_{68}^{15}$, and this large value could have its origin in partial

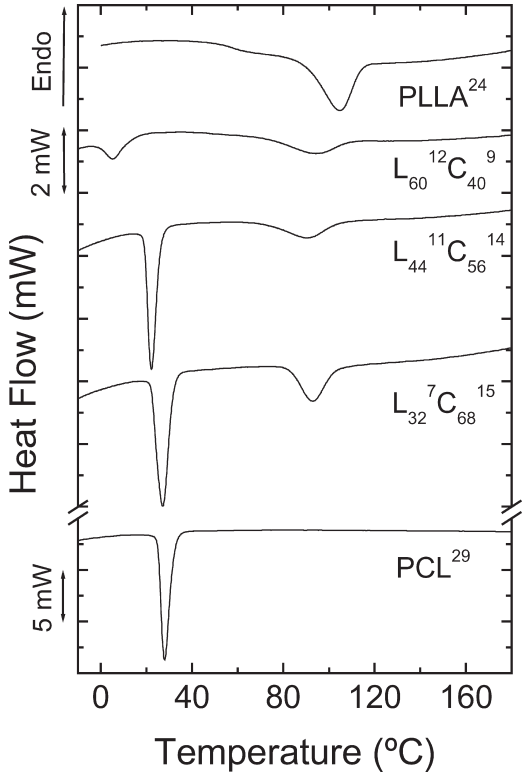

Figure 1. DSC cooling scans at 10 °C · min^{-1}, after melting at 190 °C for 3 min.

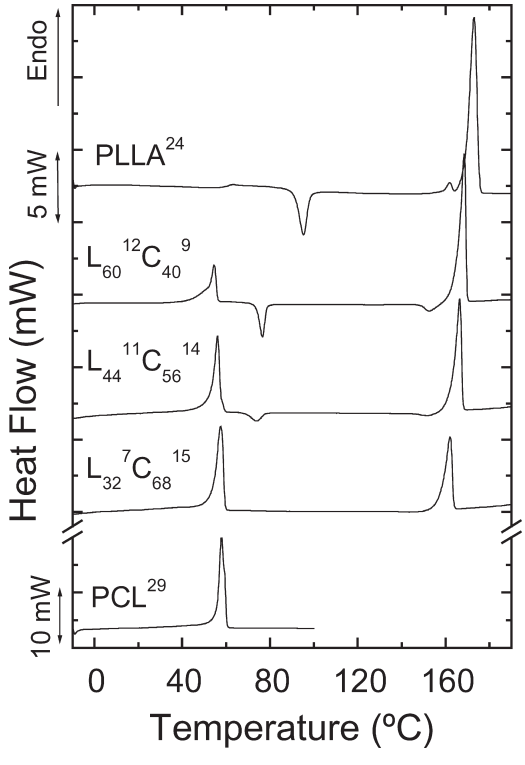

Figure 2. DSC heating scans (at 10 °C · min^{-1}) following the cooling scans presented in Figure 1.

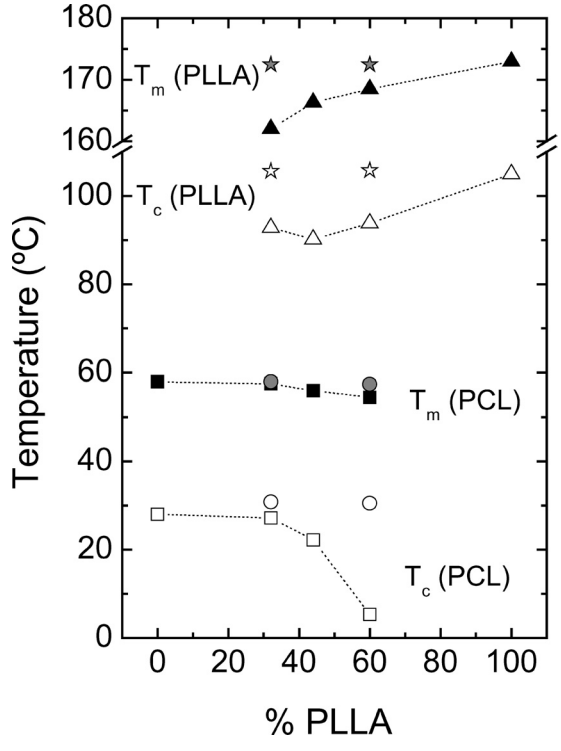

Figure 3. Melting and crystallization temperatures (obtained from the data reported in Figure 1 and 2) for the PLLA and PCL blocks within all copolymer versus PLLA composition (data points plus dashed line). The data points (without dashed line) indicate the transition temperatures for PLLA and PCL phases in the blends.

miscibility. Therefore, PCL may be acting as a diluent depressing both T_c and T_m of the PLLA rich phase. SAXS results to be presented below indicate that this copolymer (with the shortest PLLA block) is probably mixed in the melt.

Finally, Figure 3 also shows that the peak crystallization temperature for the PCL phase in the block copolymers decreases as the PLLA content increases. This could be a result of topological constraints since PLLA crystallizes first when the samples are cooled from the melt and in a break-out fashion whereby spherulites are formed regardless of composition.[6,16,21] A novel result to be presented below is than even with only 32% PLLA, well developed PLLA spherulites with molten PCL covalently bonded can still form. Then PCL is left to crystallize within the spatially constrained PLLA intra-spherulitic regions.

The standard DSC results indicate that there is a certain level of thermodynamic interactions between the blocks that allows PCL to act as a macromolecular diluent for PLLA, thereby depressing its melting point.

Melt Structure and Sequential Isothermal Crystallization Studies

The melt structure was studied by SAXS and the sequential isothermal crystallization of the PLLA block and then the

Table 3. Thermal properties obtained from DSC scans presented in Figure 1 and 2.

Sample	PCL					PLLA					
	T_c	T_m	ΔH_c	ΔH_m	T_g	T_c[a)]	T_c[b)]	T_m	ΔH_c[a)]	ΔH_c[b)]	ΔH_m
	°C	°C	J · g^{-1}	J · g^{-1}	°C	°C	°C	°C	J · g^{-1}	J · g^{-1}	J · g^{-1}
PLLA[24]	–	–	–	–	59.8	105.0	95.2	173.0	29	17	68
$L_{60}^{12}C_{40}^{9}$	5.3	54.5	15	36	–	93.8	76.5–152.7	168.5	22	15–6	73
$L_{44}^{11}C_{56}^{14}$	22.2	56.0	43	43	–	90.2	73.8–151.5	166.3	31	9–2	75
$L_{32}^{7}C_{68}^{15}$	27.2	57.5	44	63	–	92.8	–	162.0	51	–	80
PCL[29]	28.0	58.0	65	68	–	–	–	–	–	–	–

[a)] Values of crystallization temperatures and enthalpies of PLLA during cooling scans.
[b)] Values of crystallization temperatures and enthalpies of PLLA during heating scans.

PCL block was studied by both WAXS and DSC. Temperature profiles employed are shown in Figure 4. The dashed line in Figure 4 is the thermal program employed by us in a previous work[16] and applied here to selected samples for comparison to the new thermal profile shown as a solid line, which includes an additional melt annealing step as well as a higher isothermal crystallization temperature for each block. The new thermal profile was found to yield more information regarding the structure of the melt and its subsequent transformation. The arrows indicate the times and temperatures that we have selected for the presentation of specific ''time frames'' of data.

The melting point of both PLLA and PCL are very sensitive to degradation. In cases where we encountered degradation, we were able to see changes in both the profile of the melting endotherm and in its peak values. We did not detect any changes after the new annealing protocol employed here (Figure 4). Regarding possible transesterification reactions, we have blended PCL and PLLA without a catalyst and for temperatures lower than 200 °C, transesterification reactions are not promoted. Also, any transesterification reaction leads to interruption of crystallizable chain sequences. This is immediately reflected in the crystallization and melting behavior. Once more, after the annealing protocol employed, no changes whatsoever were observed in the thermal behavior of the samples.

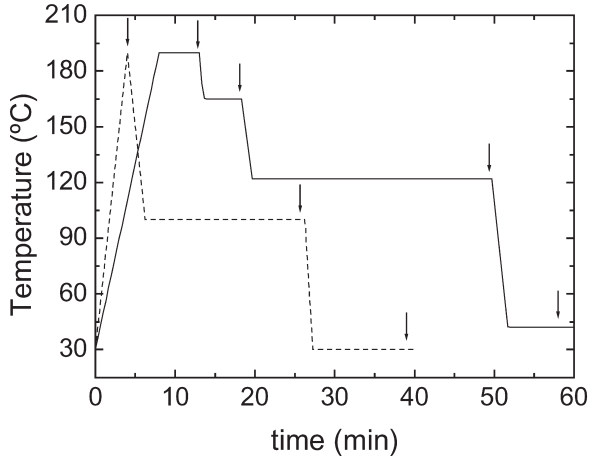

Figure 4. Temperature profiles applied during SAXS/WAXS measurements. The solid line indicated the thermal profile applied in this work. The dashed line corresponds to the thermal program employed by us in a previous work.[16] The arrows indicate the times and temperatures selected for the presentation of specific ''time frames'' of data.

Figure 5 presents DSC melting scans after the new thermal program presented in Figure 4 (solid line) was applied to the samples. For all samples except one, the melting endotherms of both blocks can be identified. We realized that the PCL block crystallization rate is slowed down so much by the previous crystallization of the PLLA block in copolymer $L_{60}^{12}C_{40}^{9}$, that at 42 °C it does not crystallize (this explains the lack of a melting endotherm in the PCL block melting temperature range in Figure 5 for this sample). This is the reason why a DSC heating scan after applying the alternate thermal program (segmented line in Figure 4) is presented in Figure 5 (labeled (a)), where a small endotherm corresponding to the melting of the PCL block crystals can be appreciated.

Before presenting time dependent X-ray data, an example of the indexation of WAXS patterns is shown in Figure 6. Similar features were observed in the WAXS patterns of all three copolymers. Representative results are presented (Figure 6) for $L_{32}^{7}C_{68}^{15}$ during a ramp in which the sample was first melted and then cooled to 100 °C, at which point PLLA crystallizes, then 30 °C at which temperature PCL crystallizes. The temperature profile corresponds to that indicated by the segmented line in Figure 4.

This allows us to identify features associated with the crystallization of the two blocks that are in agreement with data previously presented for $L_{44}^{11}C_{56}^{14}$.[16] To briefly reiterate, the following assignment is made for the peaks from crystalline PLLA: The first peak at $2\theta = 13.3°$ is assigned to the $0\bar{1}1/011$ reflections of PLLA. The very strong peak at $2\theta = 15.0°$ corresponds closely to the $110/1\bar{1}0/200$ reflections at $2\theta = 15.083$ and $15.093°$

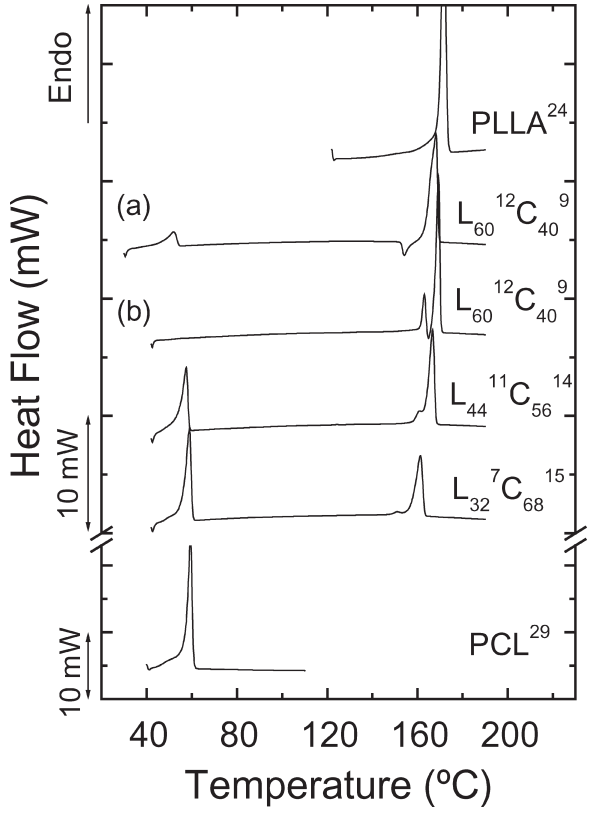

Figure 5. DSC heating scans at $10\,^{\circ}C \cdot min^{-1}$ after the main thermal program presented in Figure 4 (solid line). For the copolymer $L_{60}^{12}C_{40}^{9}$, line (a) indicated the heating scan after the thermal program presented in Figure 4 (solid line). Line (b) indicated the heating scan after the thermal program presented in Figure 4 (dashed line).

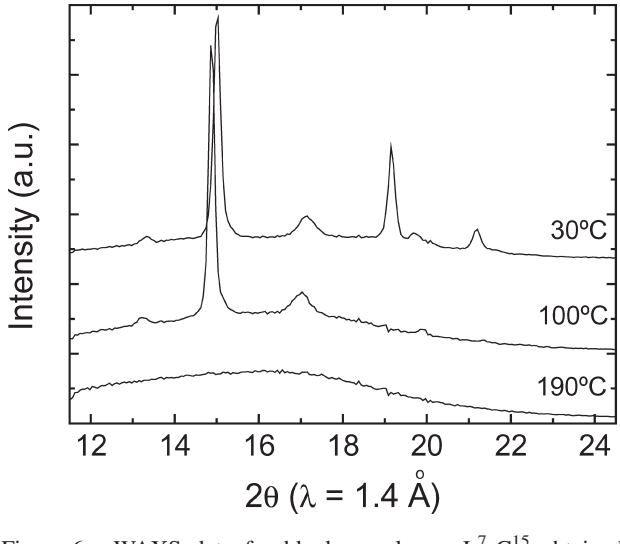

Figure 6. WAXS data for block copolymer $L_{32}^{7}C_{68}^{15}$ obtained starting at 190 °C, quenching at $50\,^{\circ}C \cdot min^{-1}$ to 100 °C where PLLA crystallizes (30 min hold), then quenching at $50\,^{\circ}C \cdot min^{-1}$ to 30 °C (15 min hold) where PCL crystallizes (segmented line in Figure 4).

respectively of the α form of PLLA (the powder diffraction pattern was calculated using the crystallographic information in ref.[26]). The next peak at $2\theta = 17.1^{\circ}$ is close to the position expected for the sets of 113 and 203 reflections of the α form of PLLA, $2\theta = 17.259^{\circ}$ and $2\theta = 17.268^{\circ}$.[26] For PCL, the reflection at $2\theta = 19.2^{\circ}$ is close to the position of the 110 reflection of PCL. The shoulder at $2\theta = 19.8^{\circ}$ may be the 111 peak, although its position is shifted from that expected ($2\theta = 20.02^{\circ}$) based on the published crystal structure.[27] The final prominent peak is the 200 peak from PCL. This data reveals a pronounced increase in the 2θ value of the PLLA peaks following crystallization of PCL. A similar feature was noted by us previously,[16] and was associated with a change in the *a* and *b* dimensions of the PLLA unit cell (i.e. a lateral contraction). This is consistent with the observation that the position of the first $(0\bar{1}1/011)$ peak does not shift significantly, a feature not previously noted.

Comprehensive SAXS data as a function of time are presented in Figure 7 for the first time for the new copolymer sample $L_{32}^{7}C_{68}^{15}$ in order to give an overview of the changes experienced by this copolymer as the main temperature program was applied (solid line in Figure 4).

Figure 8 presents selected frames of SAXS data. The SAXS profile in the melt at 190 °C, and then at 165 °C prior to PLLA crystallization are characterized by a single broad reflection. This single reflection may be interpreted as arising from a homogeneous melt in $L_{32}^{7}C_{68}^{15}$, especially if the DSC results presented in Figure 1–3 are taken into account. This may be a result of this being the sample that contains the shortest PLLA block of the three PLLA-*b*-PCL diblock copolymers employed here and therefore the one with the lowest χN value. The intensity change on crystallization most probably reflects a change in electron

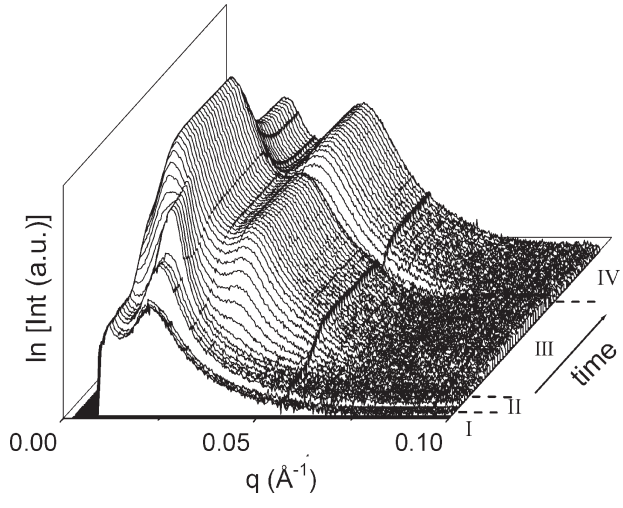

Figure 7. SAXS data for block copolymer $L_{32}^{7}C_{68}^{15}$ obtained during the temperature ramp shown in Figure 4 (solid line). The temperature regions are indicated as: I (190 °C); II (165 °C); III (122 °C) and IV (42 °C).

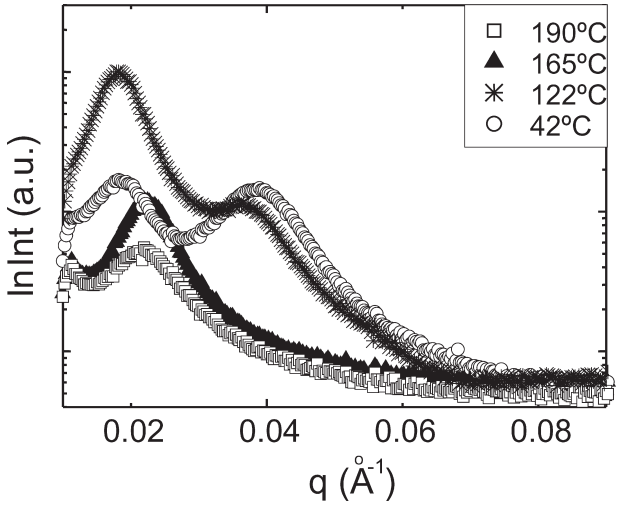

Figure 8. Selected frames (indicated by arrows in Figure 4, solid line) of SAXS data for block copolymer $L_{32}^{7}C_{68}^{15}$.

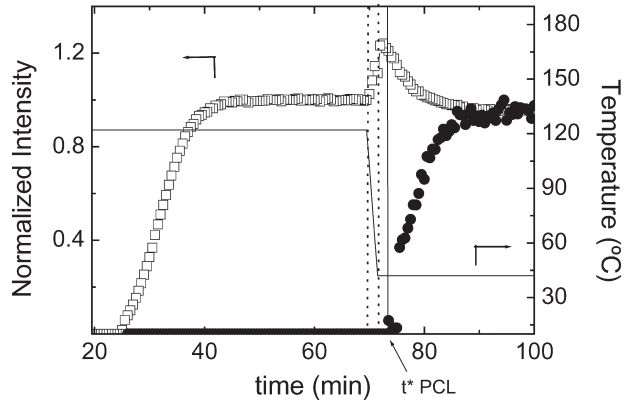

Figure 9. Normalized height of WAXS peaks for block copolymer $L_{32}^{7}C_{68}^{15}$ from fitted Lorentzian functions: (□) $2\theta = 14.8^{\circ}$ reflection of PLLA, (●) 110 reflection of PCL. The solid line indicates the temperature measured by the DSC instrument (Linkam) employed in the X-ray set-up. The dashed line indicates the cooling region from 122 to 42 °C. The vertical solid line indicates the start of PCL crystallization (t^*_{PCL}).

density profile along the lamellar normal. PCL crystallization induces a further change in the electron density profile as the intensity of first and second order reflections is reversed. However, the peak positions remain approximately the same. This suggests that PCL is crystallizing within the existing PLLA lamellae. This was also observed by Nojima et al. for PE-*b*-PCL (PE: polyethylene) diblocks crystallized at low T_c.[28] However, they reported that crystallization of PCL at high T_c led to disruption of the PE lamellae.

Upon PLLA crystallization at 122 °C, a lamellar structure develops with peak positions in the ratio 1:2 (see Figure 8). Later, upon PCL crystallization (at 42 °C), a change in peak intensities is noted, pointing to a significant variation in the lamellar crystal stacking. Figure 9 shows the corresponding WAXS data for $L_{32}^{7}C_{68}^{15}$, which shows a clear change in the intensity of the strongest reflection from PLLA upon crystallization of PCL. In fact, careful inspection of Figure 9 indicates that the initial increase in intensity after PLLA has crystallized (at approximately 70 min) coincides with the onset of cooling, from 122 down to 42 °C (see temperature ramp also in Figure 9) and could correspond to residual crystallization of PLLA facilitated by the applied supercooling. As soon as the PCL starts to crystallize (a few seconds after the temperature reaches 42 °C at t^*_{PCL}), a drop in intensity occurs that levels off when the PCL crystallization has apparently saturated. A similar effect was also previously found for $L_{44}^{11}C_{56}^{14}$ and $L_{60}^{12}C_{40}^{9}$ in our preceding work.[16] A rearrangement of the PLLA crystal stems to accommodate the crystallization of the previously amorphous PCL lamellar microdomains may be causing some level of local melting at the interphases that is capable of reducing the WAXS intensity of the strongest PLLA reflection. Another possibility that may explain the above results is that a change in the structure factor (F_{hkl}), which is proportional to the WAXS intensity, could occur since the unit cell is being distorted. It should be recalled however that as mentioned above SAXS indicates that the lamellar spacing does not change significantly upon PCL crystallization.

Figure 10 shows a superposition of WAXS and DSC data corresponding to the isothermal crystallization of PLLA at 122 °C, the agreement is good considering the intrinsic differences in the techniques. The application of the Avrami theory to the DSC data will be discussed below after the results for all samples have been presented.

Figure 11 presents optical micrographs obtained by POM during isothermal treatments at the indicated temperatures. In the case of $L_{32}^{7}C_{68}^{15}$ the same thermal protocol applied to samples examined by SAXS/WAXS was applied (solid line in Figure 4). At 122 °C the well developed negative spherulitic texture (for sign assignment, please see our

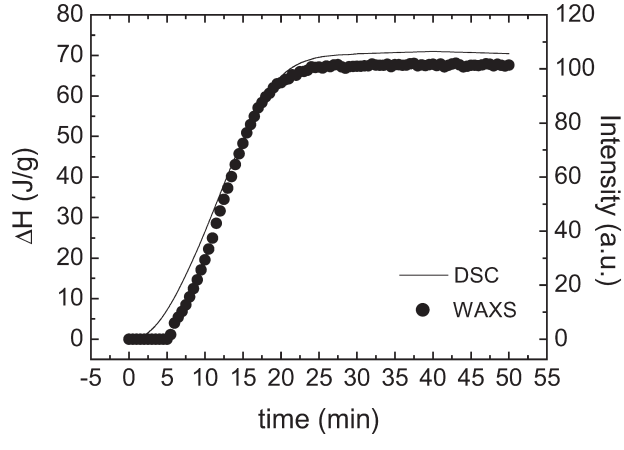

Figure 10. WAXS (data points) and DSC (solid line) data corresponding to the isothermal crystallization of the PLLA block within copolymer $L_{32}^{7}C_{68}^{15}$ at 122 °C.

previous study, ref.[16]) of PLLA can be appreciated. It is remarkable that with only 32% PLLA, $L^{7}_{32}C^{15}_{68}$ can also form well developed spherulites (with a clear Maltese cross) where the covalently bonded PCL block remains amorphous and located in the intra-spherulitic regions as intercalated lamellae. When the temperature is dropped to 42 °C, PCL crystallizes within the PLLA spherulites, and in Figure 11, only a change in the birefringence can be appreciated while the negative sign of the spherulite remains unaltered, as indicated by the colors of the quadrants. These results confirm those previously obtained by us with PLLA rich diblock copolymers.[16] For comparison purposes, a micrograph of homo-PCL crystallizing at 42 °C is presented in Figure 11.

The next sample examined by SAXS turned out to be well structured in the melt as indicated in Figure 12 where two time frames have been selected for $L^{11}_{44}C^{14}_{56}$, in the melt at 190 °C and 1.5 min after reaching 122 °C (before PLLA crystallization has started). The melt structure is lamellar since in addition to the sharp primary peak at q^* there is a second order reflection at $2q^*$. An additional shoulder at low q is evident in the melt and crystal states that seem to reflect a secondary population of lamellae (the ''peak'' at lowest q is the beamstop). The precise origin of this is at present unclear. The main reflections at q^* and $2q^*$ are much more pronounced on supercooling to 122 °C, prior to crystallization of PLLA, where even a $3q^*$ reflection can be seen. It may be that longer annealing times are needed in order to obtain even better segregated structures in the melt. However, the susceptibility of these samples to degradation does not allow this possibility to be further explored.

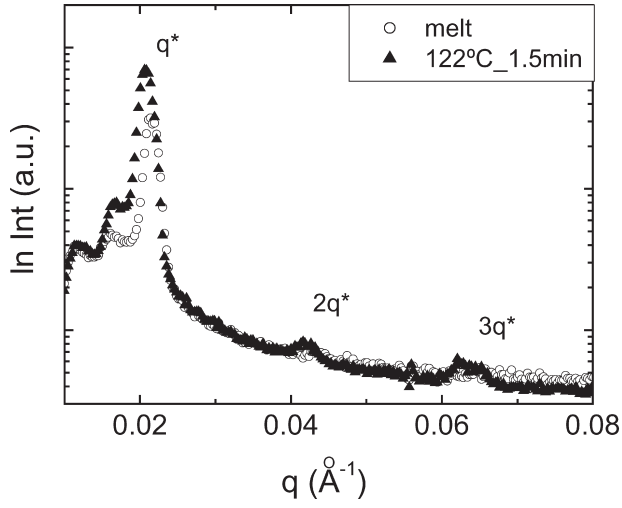

Figure 12. Selected frames of SAXS data for block copolymer $L^{11}_{44}C^{14}_{56}$ showing the higher order reflections of a lamellar structure.

Figure 13 shows that after the crystallization of PLLA at 122 °C, the diffraction peaks change completely into a diffuse scattering peak located at a lower q (plus a shoulder at almost $2q^*$), indicating that the microdomain structure has been transformed by the PLLA spherulite formation

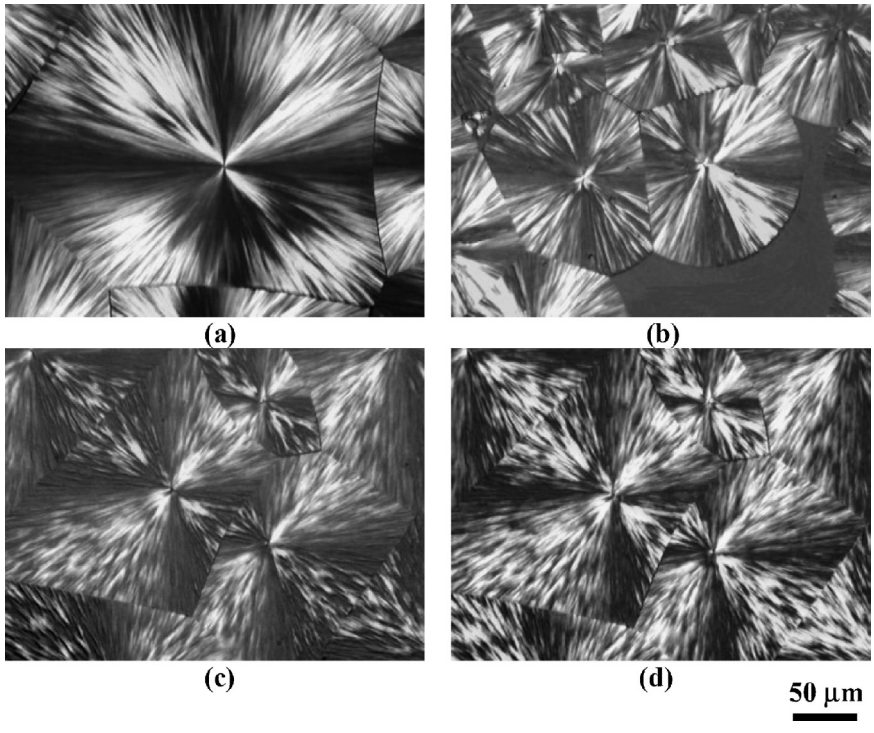

Figure 11. Polarized Optical Micrographs during isothermal crystallization: (a) homo-PLLA, after 8 min at 122 °C. (b) homo-PCL, after 10 min at 42 °C. (c) $L^{7}_{32}C^{15}_{68}$ after 30 min at 122 °C. (d) $L^{7}_{32}C^{15}_{68}$ after 15 min at 42 °C.

(also observed by POM, results not shown. See ref.[16] for images of spherulites of this copolymer obtained at 100 and 120 °C), which indicates that the driving force of crystallization overwhelmed the stability of the microdomain structure in the melt. Crystallization of PCL at 42 °C leads to a dramatic change in the lamellar morphology, as revealed by SAXS. The lower q peak decreases in intensity and the one near $2q^*$ develops from a shoulder into a much more intense and well defined peak. The peak positions are essentially unaltered. This indicates that PCL is crystallizing within pre-existing PLLA lamellae, leading to a large change in density profile. These observations are similar to those made for $L_{32}^{7}C_{68}^{15}$ as discussed above.

Figure 14 contains WAXS data showing the intensity of the main PLLA reflection at $2\theta(\lambda = 1.4\ \text{Å}) = 15.0^\circ$, and the 111 peak of PCL during a different cooling protocol, in which the melt annealing stage was omitted and the isothermal crystallization temperatures for PLLA and PCL were 100 °C and 30 °C respectively (segmented line in Figure 4). The peak positions were determined by fitting to Lorentzian functions.[16] Inspection of the data and repeated fits with different parameters confirmed the existence of the noticeable intensity jump for the PLLA $110/1\bar{1}0/200$ peak at the point of crystallization of PCL. Small, but measurable, shifts in PLLA peak position from 14.9 to 15.0° were also noted. The data using the other thermal protocol was also collected and yielded similar results but with smaller changes. The agreement between WAXS and DSC as regards the crystallization kinetics of the PLLA component at 100 °C was demonstrated previously.[16]

Copolymer $L_{60}^{12}C_{40}^{9}$ also crystallizes from an ordered lamellar melt, as shown by the SAXS data in Figure 15. The SAXS profile shows a single sharp peak at 190 °C that grows in intensity upon cooling to 165 °C. We previously interpreted similar results on the same sample (see ref.[16]) as a transient lamellar phase, but now describe this sample as weakly ordered in the melt. The lamellar ordering this time is better, a fact that could be related to the longer annealing times employed while the sample was in the melt (compare both thermal protocols in Figure 4). At 42 °C the PCL is not able to crystallize within the time frame of the experiment, this is why the SAXS pattern is identical to that taken at 122 °C after PLLA crystallization. Figure 16 shows that when the sample is cooled to 30 °C the SAXS pattern taken after 30 min is quite distinct indicating PCL crystallization.

Finally, Figure 17 again shows the very good agreement obtained by WAXS and DSC on the isothermal crystallization kinetics of the PLLA block at 122 °C within $L_{60}^{12}C_{40}^{9}$.

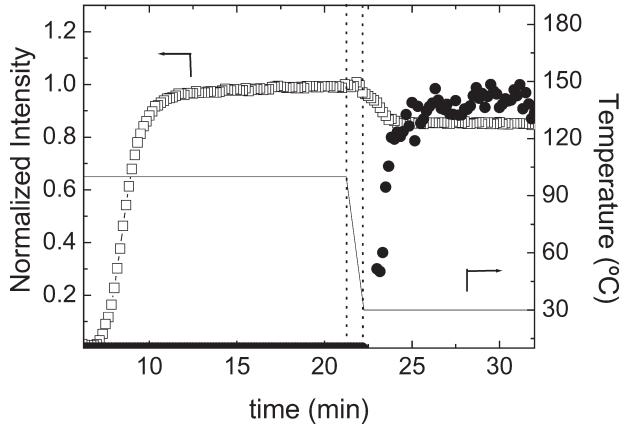

Figure 14. Normalized height of WAXS peaks for block copolymer $L_{44}^{11}C_{56}^{14}$ from fitted Lorentzian functions: (□) $2\theta = 14.8^\circ$ reflection of PLLA, (●) 110 reflection of PCL. The solid line indicates the temperature measured by the DSC instrument (Linkam) employed in the X-ray set-up. The dashed line indicated the cooling region from 122 to 42 °C.

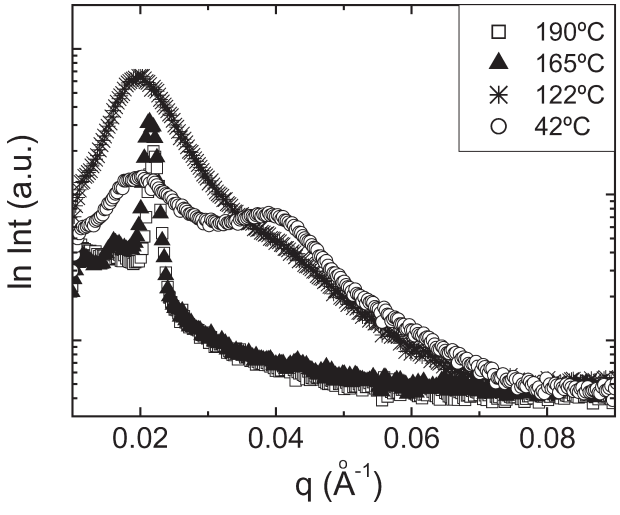

Figure 13. Selected frames (indicated by arrows in Figure 4, solid line) of SAXS data for block copolymer $L_{44}^{11}C_{56}^{14}$.

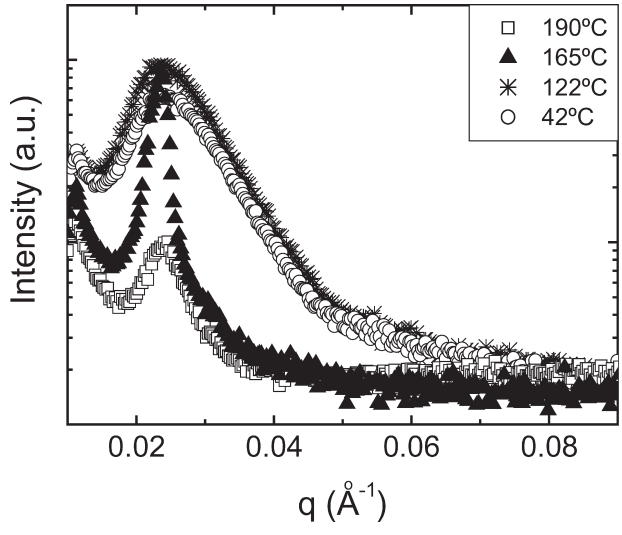

Figure 15. Selected frames (indicated by arrows in Figure 4, solid line) of SAXS data for block copolymer $L_{60}^{12}C_{40}^{9}$.

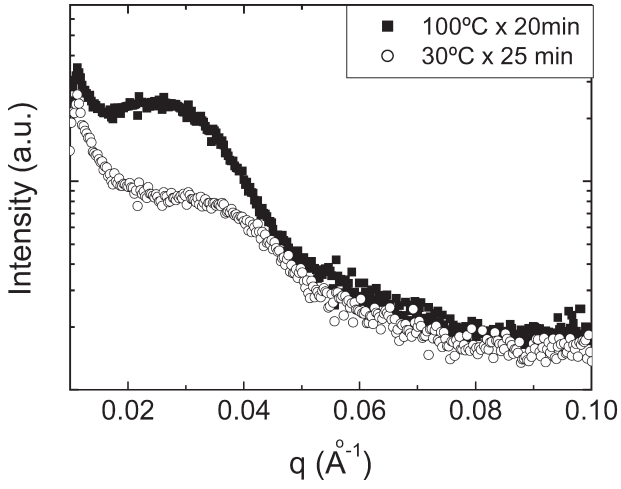

Figure 16. Selected frames of SAXS data for block copolymer $L_{60}^{12}C_{40}^{9}$ obtained during the temperature ramp shown in Figure 4 (dashed line).

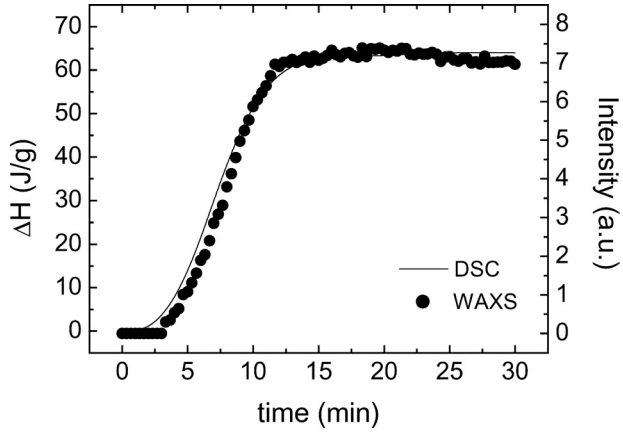

Figure 17. WAXS (data points) and DSC (solid line) data corresponding to the isothermal crystallization of PLLA block within $L_{60}^{12}C_{40}^{9}$ copolymer at 122 °C.

Table 4 presents results on the application of the Avrami crystallization equation to fit the isothermal crystallization data obtained by DSC as detailed previously (see ref.[16]). Several interesting observations can be made from the results. The overall crystallization rate of the PLLA block as compared to PLLA homopolymer at a constant temperature of 122 °C (i.e., a temperature where the PCL block is molten) is slowed down by the incorporation of 40% covalently bonded PCL. When the amount of PCL is 56% the rate goes down even more (or conversely, the half-crystallization time increases), but seems to saturate since further increases of PCL to 68% leave the overall crystallization rate unaffected. Similar results where a crystallizable block is affected by a second rubbery block during isothermal crystallization has been reported by some of us for PPDX-*b*-PCL diblock copolymers.[7,12] In addition, the Avrami index corresponding to the PLLA block is progressively lower in the copolymers as the PCL content increases, nevertheless it remains between 2 and 3. The physical meaning of this reduction is difficult to explain because it cannot be connected to growth dimensionality since in all cases spherulites were observed.

The case of the PCL block is interesting, since its overall crystallization kinetics were measured after the PLLA was crystallized until saturation (Figure 4). Since we observed by POM that PLLA spherulites grew and impinged at 122 °C (see Figure 11 and ref.[16]), it is clear that upon cooling PCL had to crystallize within the PLLA spherulites with an obvious effect on crystallization rate. The results are therefore expected. The half-crystallization time increased with PLLA content, however, when the PLLA content reached 60%, the PCL block was not able to crystallize at all within the time frame of the experiment. As a reference, some values obtained at a lower crystallization temperature (at 30 °C) are presented in Table 4. When the Avrami index is compared for the samples that did crystallize at 42 °C, a reduction in its value was also obtained as compared to homo-PCL (for which a value close to 3 was obtained, i.e., 2.89). This reduction may be connected with topological restrictions that may hinder three- dimensional growth.

Table 4. Avrami parameters obtained by fitting isothermal crystallization data obtained by DSC.

Sample	PCL ($T_c = 42$ °C)				PLLA ($T_c = 122$ °C)			
	n	K / min^{-n}	$\tau_{50\%}$ / min	R^2	n	K / min^{-n}	$\tau_{50\%}$ / min	R^2
PLLA[24]	–	–	–	–	2.85	0.0082	4.75	1
$L_{60}^{12}C_{40}^{9}$	2.39[a)]	0.0035[a)]	9.15[a)]	0.9999[a)]	2.56	0.0048	6.88	0.9999
$L_{44}^{11}C_{56}^{14}$	1.97	0.0023	18.27	0.9998	2.21	0.0030	11.35	0.9999
$L_{32}^{7}C_{68}^{15}$	1.55	0.0265	8.62	0.9997	2.03	0.0049	11.30	1
PCL[29]	2.89	0.0019	7.85	1	–	–	–	–

[a)] The PCL block in this copolymer was crystallized at 30 °C after the previous crystallization of the PLLA block (see text).

It should be noted that the molecular weight of the homopolymer analogues is somewhat higher than that corresponding to each component within the block copolymers. If there would be an influence in this molecular weight range over crystallization kinetics, it would be that as $\overline{M}_n$ decreases, the crystallization rate should be higher. Since we found a decrease in the crystallization rate of each block component as compared to the homopolymer analogue, this means the effect observed is even stronger if the molecular weight differences were to cause a significant effect. In other words, in this case the molecular weight differences are either not causing an effect or they are being overwhelmed by the topological restrictions that the chains encounter by being tethered to another block component.

Conclusion

We have investigated the sequential crystallization of three PLLA-*b*-PCL diblock copolymers $L^{7}_{32}C^{15}_{68}$, $L^{11}_{44}C^{14}_{56}$ and $L^{12}_{60}C^{9}_{40}$. The crystallization of the sample with the shortest PLLA block ($L^{7}_{32}C^{15}_{68}$) proceeds from a disordered melt. Crystallization of PLLA leads to a lamellar crystal structure, as revealed by WAXS. The subsequent isothermal crystallization of PCL at 42 °C leads to a rearrangement of the lamellar superstructure, together with a change in PLLA unit cell parameters (WAXS peak position shift and intensity change). We have established by employing a new thermal annealing protocol during real time SAXS experiments that both $L^{11}_{44}C^{14}_{56}$ and $L^{12}_{60}C^{9}_{40}$ diblocks crystallize from lamellar microphase separated melts, which form on supercooling. The microphase structure of the melt is changed as PLLA crystallizes at 122 °C (a temperature at which the PCL block is molten) forming spherulites regardless of composition (even with only 32% PLLA, a novel result). SAXS indicated that a lamellar structure with a different periodicity than that obtained in the melt forms for sample $L^{11}_{44}C^{14}_{56}$. For this sample, in which PLLA is the minority block, PCL crystallization changes the already formed PLLA crystal structure, at the level of the crystal lamellae and the crystal unit cell. In contrast, for sample $L^{12}_{60}C^{9}_{40}$, PCL does not crystallize at 42 °C, so there is no change in PLLA crystal structure. Crystallization is observed by DSC and SAXS at lower temperatures (30 °C). The crystallization kinetics of PLLA for all three samples measured by DSC and WAXS were compared and found to be in good agreement. The crystallization kinetics of both blocks were studied by DSC. The crystallization of PLLA is slowed down by incorporation of PCL, and the Avrami exponent decreases (although a spherulitic structure is retained). The crystallization of PCL is also slowed down in the diblocks compared to the homopolymer, and the Avrami exponent is reduced even more strongly than for PLLA. These results show that the crystallization structure, thermodynamics and kinetics of the biodegradable PLLA block can be influenced by coupling to biodegradable PCL in double crystalline diblock copolymers in which sequential crystallization occurs on cooling.

Acknowledgements: This work was supported by *EPSRC* grant GR/ S73037/01. X-ray data peak fitting program xfit is provided by *CCP13*, the collaborative project for fiber diffraction data analysis. The *USB team* acknowledges sponsorship by *Fonacit* (grant No. S1-2001000742).

[1] I. W. Hamley, *The Physics of Block Copolymers*, Oxford University Press, Oxford 1998.
[2] I. W. Hamley, *Adv. Polym. Sci.* **1999**, *148*, 113.
[3] Y. L. Loo, R. A. Register, ''Crystallization Within Block Copolymer Mesophases'', in: *Developments in Block Copolymer Science and Technology*, I. W. Hamley, Ed., Wiley, New York 2004, p. 213.
[4] A. J. Müller, V. Balsamo, M. L. Arnal, *Adv. Polym. Sci.* **2005**, *190*, 1.
[5] Y. K. Choi, Y. H. Bae, S. W. Kim, *Macromolecules* **1998**, *31*, 8766.
[6] J. K. Kim, D. J. Park, M. S. Lee, K. J. Ihn, *Polymer* **2001**, *42*, 7429.
[7] J. Albuerne, L. Marquez, A. J. Müller, J. M. Raquez, P. Degee, P. Dubois, V. Castelletto, I. W. Hamley, *Macromolecules* **2003**, *36*, 1633.
[8] N. Bhattarai, H. Y. Kim, D. I. Cha, D. R. Lee, D. I. Yoo, *Eur. Polym. J.* **2003**, *39*, 1365.
[9] R.-M. Ho, P.-Y. Hsieh, W.-H. Tseng, C.-C. Lin, B.-H. Huang, B. Lotz, *Macromolecules* **2003**, *36*, 9085.
[10] G. Maglio, A. Migliozzi, R. Palumbo, *Polymer* **2003**, *44*, 369.
[11] A. J. Müller, J. Albuerne, L. M. Esteves, L. Márquez, J. M. Raquez, P. Degée, P. Dubois, S. Collins, I. W. Hamley, *Macromol. Symp.* **2004**, *215*, 369.
[12] A. J. Müller, J. Albuerne, L. Márquez, J. M. Raquez, P. Degée, P. Dubois, J. Hobbs, I. W. Hamley, *Faraday Discuss.* **2004**, *128*, 231.
[13] S. Nojima, Y. Akutsu, A. Washino, S. Tanimoto, *Polymer* **2004**, *45*, 7317.
[14] L. Sun, Y. Liu, L. Zhu, B. S. Hsiao, C. A. Avila-Orta, *Polymer* **2004**, *45*, 8181.
[15] S. Jiang, H. Chaoliang, L. An, X. Chen, B. Jiang, *Macromol. Chem. Phys.* **2004**, *205*, 2229.
[16] I. W. Hamley, V. Castelletto, R. V. Castillo, A. J. Müller, C. M. Martin, E. Pollet, P. Dubois, *Macromolecules* **2005**, *38*, 463.
[17] R. Dell'Erba, G. Groeninckx, G. Maglio, M. Malinconico, A. Migliozzi, *Polymer* **2001**, *42*, 7831.
[18] Y.-H. Na, Y. He, X. Shuai, Y. Kikkawa, Y. Doi, Y. Inoue, *Biomacromolecules* **2002**, *3*, 1179.
[19] J. M. Yang, H. L. Chen, J. W. You, J. C. Hwang, *Polym. J.* **1997**, *29*, 657.
[20] Z.-G. Wang, X. Wang, B. S. Hsiao, S. Andjelić, D. Jamiolkowski, J. McDivitt, J. Fischer, J. Zhou, C. Han, *Polymer* **2001**, *42*, 8965.
[21] O. Jeon, S.-H. Lee, S. H. Kim, Y. M. Lee, Y. H. Kim, *Macromolecules* **2003**, *36*, 5585.

[22] D. Garlotta, *J. Polym. Environ.* **2001**, *9*, 63.
[23] P. Dubois, C. Jacobs, R. Jerome, P. Teyssie, *Macromolecules* **1991**, *24*, 3027.
[24] C. C. Tang, C. M. Martin, D. Laundy, G. P. Diakun, *Nucl. Instrum. Methods Phys. Res., Sect. B* **2004**, *222*, 659.
[25] R. J. Cernik, P. Barnes, G. Bushnell-Wye, A. J. Dent, G. P. Diakun, J. V. Flaherty, G. N. Greaves, E. L. Heeley, W. Helsby, S. D. M. Jacques, J. Kay, T. Rayment, A. J. Ryan, C. C. Tang, N. J. Terrill, *J. Synchrotron Rad.* **2004**, *11*, 163.
[26] S. Sasaki, T. Asakura, *Macromolecules* **2003**, *36*, 8385.
[27] Y. Chatani, Y. Okita, H. Tadokoro, Y. Yamashita, *Polym. J.* **1970**, *1*, 555.
[28] S. Nojima, Y. Akutsu, M. Akaba, S. Tanimoto, *Polymer* **2005**, *46*, 4060.

